

## SEISMIC FAULT MODEL FOR PREDICTING STRONG GROUND MOTIONS BASED ON PHYSICAL RELATION BETWEEN SURFACE AND SUBSURFACE SLIP

Kiyoshi IRIE<sup>1</sup>, Kazuo DAN<sup>1</sup>, Ryoichiro MATSUMOTO<sup>1</sup>,  
Masayuki MIAKE<sup>2</sup> and Kojiro IRIKURA<sup>3</sup>

<sup>1</sup> Ohsaki Research Institute, Inc., 2-2-2 Uchisaiwai-cho, Chiyoda-ku, Tokyo, 100-0011, Japan

<sup>2</sup> The Japan Atomic Power Company, 1-1 Kanda-Mitoshiro-cho, Chiyoda-ku, Tokyo, 101-0053, Japan

<sup>3</sup> Aichi Institute of Technology, 1247 Yachigusa, Yakusa-cho, Toyota-shi, Aichi, 470-0392, Japan

Email: k.irie@ohsaki.co.jp, dan@ohsaki.co.jp, matsumotor@ohsaki.co.jp,  
masayuki-miake@japc.co.jp, irikura@geor.or.jp

### ABSTRACT :

The strong ground motions and the displacement of the surface fault trace are the results of the rupture of the subsurface fault, but they are not related physically with each other so far. Therefore, we proposed a procedure to model a subsurface fault for predicting strong ground motions under the physical constraint of the displacement of the surface fault trace estimated by the empirical relationship between the fault length and the displacement.

In the procedure, given the fault length and the width, eight fault parameters of the fault area, the seismic moment, the short-period level, the average stress drop on the entire fault, the average slip on the entire fault, the area of the asperities, the stress drop on the asperities, and the *S*-wave velocity of the shallow layers were evaluated based on the eight theoretical and empirical equations of these fault parameters. Here, the short-period level is the flat level of the acceleration source spectrum in the short-period range. Since two unknown constants were included in the equations, they were determined by the results of a preliminary dynamic rupture simulation. We carried out the dynamic rupture simulation by the 3D finite difference method.

We took an example of the fault model 25-km long and 15-km wide, consisting of two asperities. And, we obtained the areas of the asperities of 3.2 km×3.2 km and 1.9 km×1.9 km, the dynamic stress drop of the asperities of 32 MPa, and the *S*-wave velocity of the shallowest layer of 0.5 km/s.

On the other hand, the rupture propagation velocity of the results was faster than the *S*-wave velocity, called super-shear, on some area of the fault. Since the super-shear rupture propagation velocity is not realistic in the earthquake of the fault size studied in this paper, we should further examine the parameters of the slip weakening model, for example, giving some random fracture energy on the fault.

### KEYWORDS:

subsurface fault, strong motion prediction, asperity model,  
dynamic rupture simulation, slip-weakening model, surface fault

## 1. INTRODUCTION

In Japan, the field exploration of the active faults and the interpretation of the exploration results have been carried out intensively since the 1995 Great Hanshin-Awaji Disaster in Hyogo-Ken-Nambu earthquake of  $M_J 7.3$ , because this crustal earthquake was caused by the well-known several active faults.

In order to apply the information of the active faults to the regional disaster mitigation and the earthquake resistant structural design, strong ground motions have been predicted in cases that large earthquakes would occur on these active faults. In predicting strong ground motions, an asperity model is often adopted, consisting of the asperities with high stress drop and the background with zero stress drop. Based on the survey of the active faults and the seismicity in the interested zone, we assume the fault length and the thickness of the

seismogenic layer, and then evaluate the fault width, the area, the seismic moment, and the short-period level. The average stress drop on the entire fault, the stress drop on the asperities, and the area of the asperities are calculated from the area, the seismic moment, the short-period level, and three equations describing the characteristics of the asperity model. The average slip on the asperities is assumed to be twice the average slip on the entire fault.

On the other hand, the displacement of the ground surface near the fault is usually evaluated under the constraint of the displacement of the surface fault trace, that is estimated by the empirical relationship of the fault length and the magnitude and that of the surface fault displacement and the magnitude.

Since the displacement of the surface fault trace and the strong ground motions are the results of the rupture of the subsurface fault, they should be related physically with each other.

Consequently, we tried to model a subsurface fault for predicting strong ground motions under the physical constraint of the displacement of the surface fault trace given by the empirical relationship between the fault length and the surface fault displacement.

## 2. RELATIONSHIPS AMONG FAULT PARAMETERS

The subsurface fault model is described by ten main parameters of the fault length  $L$ , the width  $W$ , the area  $S$ , the seismic moment  $M_0$ , the short-period level  $A$ , the average stress drop on the entire fault  $\Delta\sigma$ , the average slip on the entire fault  $D$ , the area of the asperities  $S_{asp}$ , the stress drop on the asperities  $\Delta\sigma_{asp}$ , and the average slip on the asperities  $D_{asp}$ . After  $L$  and  $W$  are given, other eight parameters are evaluated by the following five theoretical equations (2.1) to (2.5) and three empirical equations (2.6) to (2.8):

$$S = LW, \quad (2.1)$$

$$\Delta\sigma = (7/16)M_0/(S/\pi)^{1.5}, \quad (2.2)$$

$$M_0 = \mu DS, \quad (2.3)$$

$$S\Delta\sigma = S_{asp}\Delta\sigma_{asp}, \quad (2.4)$$

$$A = 4\pi(S_{asp}/\pi)^{1/2}\Delta\sigma_{asp}\beta^2, \quad (2.5)$$

$$S[\text{km}^2] = 4.24 \times 10^{-11} \times (M_0[\text{dyne} \cdot \text{cm}])^{1/2}, \quad (2.6)$$

$$A[\text{dyne} \cdot \text{cm/s}^2] = 2.46 \times 10^{17} \times (M_0[\text{dyne} \cdot \text{cm}])^{1/3}, \quad (2.7)$$

$$D_{asp} = 2.01D. \quad (2.8)$$

Equation (2.6) is the empirical relationship between the fault area  $S$  and the seismic moment  $M_0$  for large earthquakes proposed by Irikura and Miyake (2001). Figure 1 shows this relationship and another relationship proposed by Somerville *et al.* (1999) with the data by Somerville *et al.* (1999) and Stirling *et al.* (2002). Equation (2.7) is the empirical relationship between the short-period level  $A$  and the seismic moment  $M_0$  proposed by Dan *et al.* (2001). Figure 2 shows this relationship with the data by Dan *et al.* (2001). Equation (2.8) shows the relationship between the average slip on the asperities  $D_{asp}$  and the average slip on the entire fault  $D$  proposed by Somerville *et al.* (1999). Figure 3 shows this relationship and the data by Somerville *et al.* (1999).

On the other hand, Matsuda (1975) proposed the empirical relationship between the fault length  $L_{ma}$  and the magnitude  $M$  described by equation (2.9) and that between the displacement of the fault trace  $D_{ma}$  and the magnitude described by equation (2.10) proposed Matsuda (1975). Equation (2.9) and (2.10) lead to equation (2.11), relating  $D_{ma}$  and  $L_{ma}$ . Figure 4 shows the equation (2.11) and the data by Matsuda (1975).

$$\log L_{ma}[\text{km}] = 0.6M - 2.9 \quad (2.9)$$

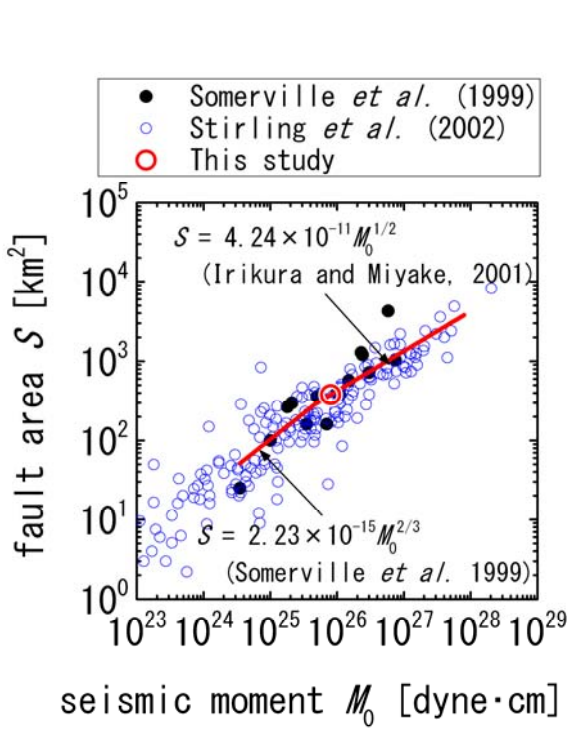


Figure 1 Relationship between the seismic moment and the fault area

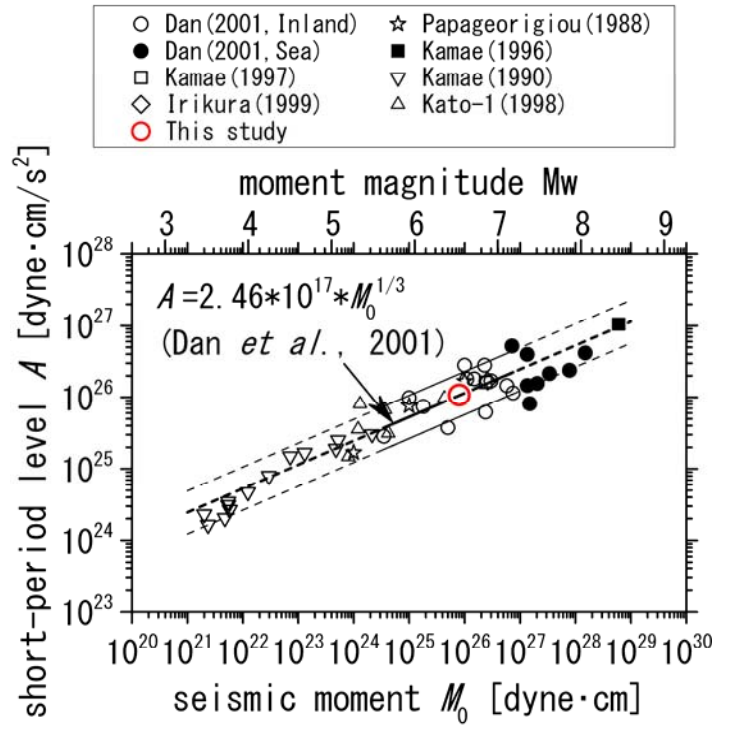


Figure 2 Relationship between the seismic moment and the short-period level

$$\log D_{ma}[\text{m}] = 0.6M - 4.0 \quad (2.10)$$

$$D_{ma}[\text{m}] = 0.0794L_{ma}[\text{km}] \quad (2.11)$$

When we model a subsurface fault for predicting strong ground motions under the physical constraint of the displacement of the surface fault trace given based on the empirical relationship between the fault length and the surface fault displacement, we should exclude equations (2.2) and (2.8). This is because equation (2.2) describes the average stress drop of a circular crack buried in the seismogenic layer and it might not be able to applied to the fault with the rupture reaching the surface. And, this is because equation (2.8) describes the average slip on the asperities obtained from kinematic fault models and these asperities might not the asperities with the high stress drop in a dynamic fault model.

Hence, in this paper, we introduced the following two equations, given  $L$  and  $W$ :

$$M_0 = l\Delta\sigma, \quad (2.12)$$

$$D_{ma} = mD\sqrt{\beta}/\sqrt{\beta_1}. \quad (2.13)$$

Here,  $\beta_1$  is the  $S$ -wave velocity of the shallowest layer, and we assume that the  $S$ -wave velocities of the layers above the seismogenic layer change linearly.

Since two unknown constants  $l$  and  $m$  are included in the equations, they are determined by the results of a preliminary dynamic rupture simulation as follows:

$$M_0^* = l\Delta\sigma^*, \quad (2.14)$$

$$S\Delta\sigma^* = S_{asp}^*\Delta\sigma_{asp}^*, \quad (2.15)$$

$$D_{ma}^* = mD^* \sqrt{\beta} / \sqrt{\beta_1^*}. \quad (2.16)$$

Here,  $S_{asp}^*$ ,  $\Delta\sigma_{asp}^*$ , and  $\beta_1^*$  are the input data, and  $M_0^*$  and  $D_{ma}^*$  are the simulation results. Consequently, given the fault length and the width, eight fault parameters of the fault area  $S$ , the seismic moment  $M_0$ , the short-period level  $A$ , the average stress drop on the entire fault  $\Delta\sigma$ , the average slip on the entire fault  $D$ , the area of the asperities  $S_{asp}$ , the stress drop on the asperities  $\Delta\sigma_{asp}$ , and the  $S$ -wave velocity of the shallowest layer  $\beta_1$  were evaluated based on the eight theoretical and empirical equations of (2.3) to (2.7) and (2.11) to (2.13).

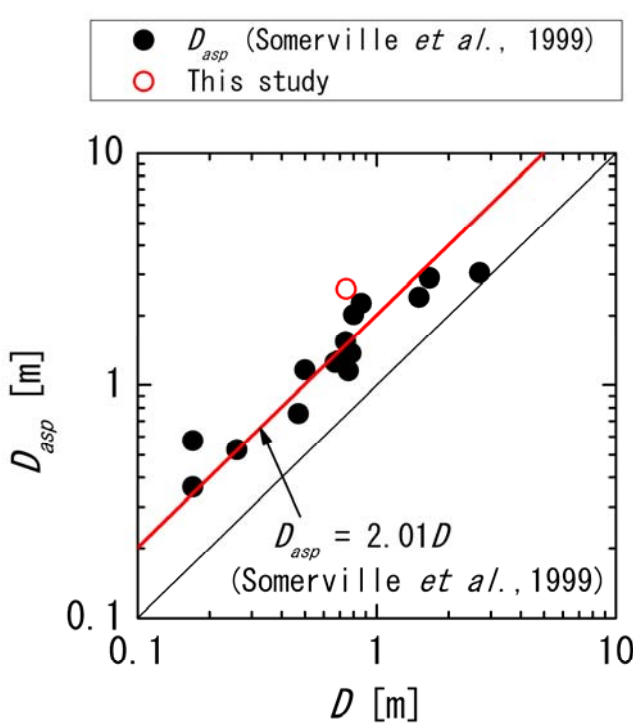


Figure 3 Relationship between the average slip on the fault area and the average slip on the asperity

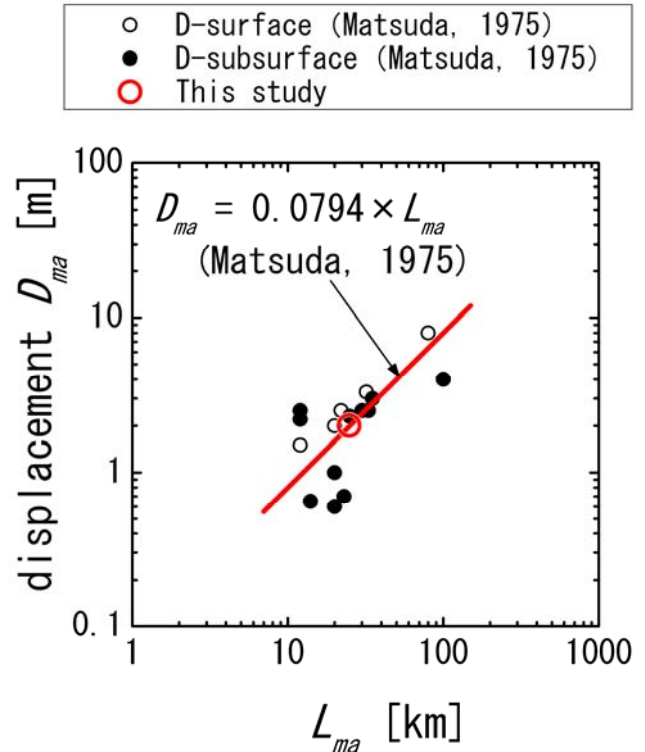


Figure 4 Relationship between the fault length and the displacement

### 3. FAULT MODEL USED IN DYNAMIC RUPTURE SIMULATION

We took an example of fault model 25-km long and 15-km wide shown in Figure 5 to show the application of the procedure described in the previous section. It had two asperities, whose area ratio was 16:6 as derived by Somerville *et al.* (1999).

The dynamic rupture simulation was performed by the 3D finite difference method program developed by Pitarka (2005). The preliminary simulation gave the constant values of  $l=6.81 \times 10^{18} \text{Nm/MPa}$  and  $m=0.926$ .

The areas of the asperities were obtained to be 3.2 km $\times$ 3.2 km and 1.9 km $\times$ 1.9 km, the stress drop on the asperities was obtained to be 32 MPa, and the  $S$ -wave velocity of the shallowest layer was obtained to be 0.5 km/s.

Figure 6 shows the slip-weakening model used as the constitutional law on the fault. Here, we assumed the values of the critical distance  $D_c$  and the strength excess  $SE$  a priori.

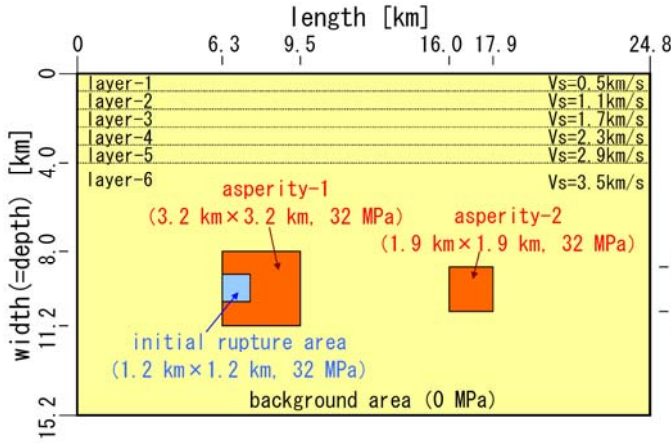


Figure 5 Fault model

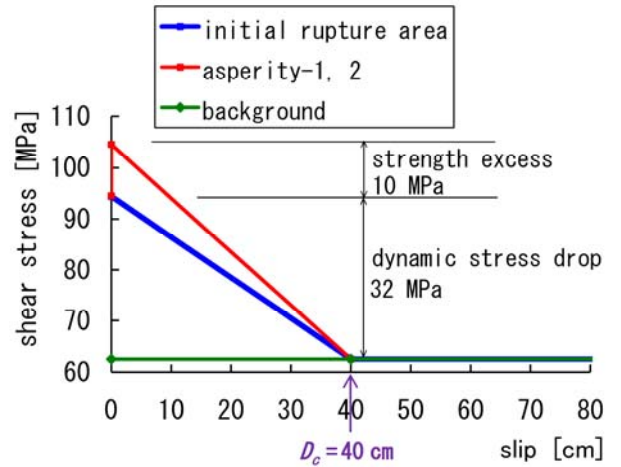


Figure 6 Slip-weakening model

#### 4. RESULTS OF DYNAMIC RUPTURE SIMULATION

Figures 7 to 10 show the results of the dynamic rupture simulation for the fault model shown in Figures 5 and 6. Figure 7 shows the final slip, indicating that the maximum slip on the ground surface  $D_{ma}$  is 2.0 m. The seismic moment  $M_0$  was calculated from the final slip by

$$M_0 = \int \mu D dS \doteq \sum_{i=1}^N \mu_i D_i \Delta S_i. \quad (4.1)$$

Here,  $\mu$  is the rigidity,  $D$  is the final slip,  $S$  is the area,  $i$  is the numbering of the sub-faults, and  $N$  is the total number of the sub-faults. The seismic moment was calculated to be  $8.00 \times 10^{18}$  Nm. Next, the short-period level  $A$  was calculated to be  $1.07 \times 10^{19}$  Nm/s<sup>2</sup> by the equation (2.5).

In Figure 1, the red circle was the fault area  $S$  and the seismic moment  $M_0$ . In Figure 2, the red circle was the seismic moment  $M_0$  and the short-period level  $A$ . In Figure 4, the red circle was the fault length  $L_{ma}$  and the maximum slip on the ground surface  $D_{ma}$ . These figures show that the dynamic fault model shown in Figures 5 and 6 reproduces the empirical relationships of the fault parameters for the actual earthquakes.

In addition, the average slip  $D_{asp}$  on the asperities shown in Figure 5 was calculated to be 2.6 m from Figure 7. In Figure 3, the red circle was the average slip on the asperities  $D_{asp}$  and the average slip on the entire fault  $D$ . This figure shows that  $D_{asp}$  is clearly longer than the empirical relationship by Somerville *et al.* (1999). This is because the empirical relationship describes the average slip on the asperities obtained from kinematic fault models, not on the asperities in dynamic fault models.

Figure 8 shows the rupture time on the fault, and it gives the rupture propagation velocities. The average rupture propagation velocity in the asperity-1 was estimated to be 4.0 km/s in the direction of mode 2 and 2.5 km/s in the direction of mode 3. On the other hand, the rupture propagation velocity in the background was estimated to be 5~6 km/s in the direction of mode 2. These rupture propagation velocities in the direction of mode 2 exceeded the  $S$ -wave velocity, called super-shear. The phenomena of the super-shear rupture velocity has been sometimes observed at megafault systems of the 1999 Izmit earthquake, the 2002 Denali earthquake, and so on. But, in the earthquakes of the fault size of this study, the super-shear rupture velocity is not realistic. Then, we should further examine the parameters of the slip weakening model in order to avoid super-shear, for example, giving some random fracture energy on the fault.

Velocity ground motions were calculated in the dynamic rupture simulation. Figure 9 shows the synthetic particle velocity motions of the horizontal components on the ground surface from the results of the dynamic rupture simulation. In Figure 9, the blue line shows the fault, and the red lines in the blue line show the surface projection of the asperities. Figure 10 shows the relationship between the shortest distance from the fault and the

peak ground velocity (PGV) of the results of the dynamic simulation in this study. In Figure 10, the red line is the empirical attenuation by Si and Midorikawa (1999). In this result, the PGV was partially higher than the empirical attenuation by Si and Midorikawa (1999). One of the reason of this high PGV might be the super-shear propagation velocity on the fault in the dynamic rupture simulation.

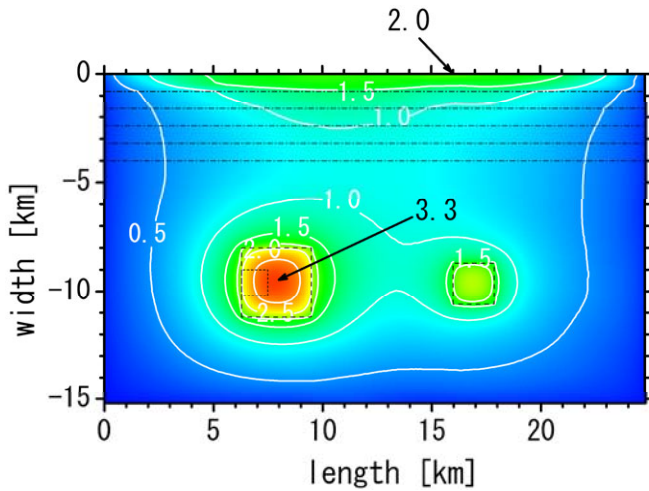


Figure 7 Resultant final slip in meters

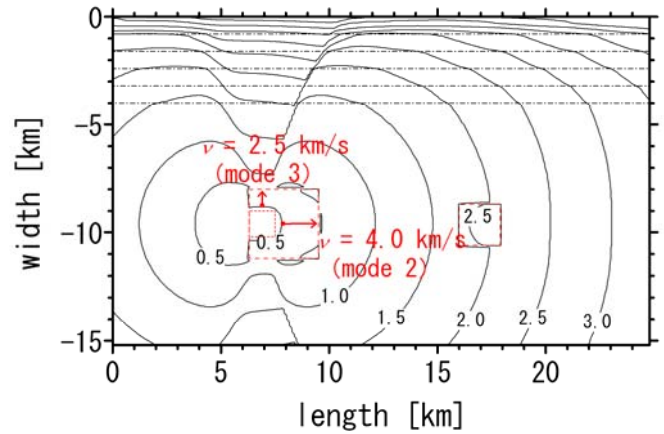


Figure 8 Resultant rupture time in seconds

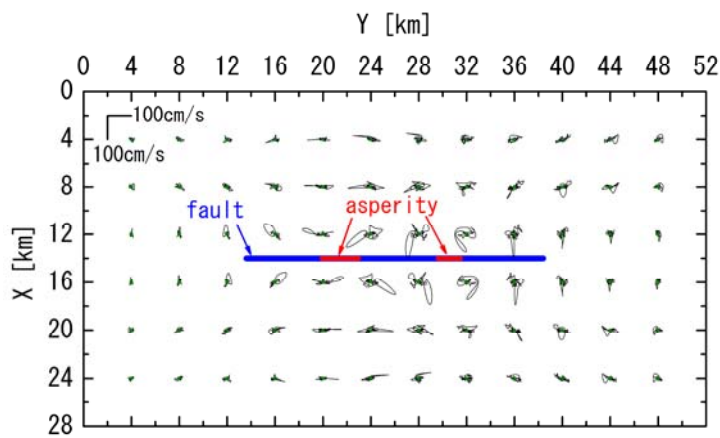


Figure 9 Resultant particle velocity motions of horizontal components on the ground surface

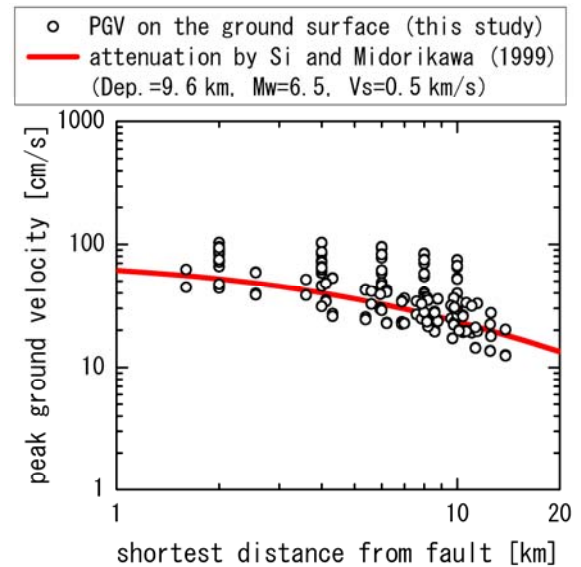


Figure 10 Comparison between the PGV in the results of this study and the attenuation by Si and Midorikawa (1999)

## 5. CONCLUSIONS

We summarize the conclusions as follows:

- 1) We could model a subsurface fault 25-km long and 15-km wide for predicting strong ground motions under the physical constraint of the displacement of the surface fault trace based on the empirical relationship between the fault length and the displacement.

- 2) Given the fault length and the width, eight fault parameters of the fault area, the seismic moment, the short-period level, the average stress drop on the entire fault, the average slip on the entire fault, the area of the asperities, the stress drop on the asperities, and the *S*-wave velocity of the shallowest layer were evaluated based on the eight theoretical and empirical equations of these fault parameters. Since two unknown constants were included in the equations, they were determined by the results of a preliminary dynamic rupture simulation.
- 3) The dynamic rupture simulation showed the super-shear rupture propagation velocity on some part of the background. We need to modify how to distribute the fracture energy on the fault such as to give some randomness to the slip-weakening law to avoid the super-shear rupture propagation velocity.
- 4) Because the application examples of the proposed procedure are limited in this paper, we need to examine various faults such as megafault systems for the next step.

## ACKNOWLEDGMENTS

We wish to express our appreciation to Dr. Pitarka at URS Corporation, USA, for his allowance of usage of his 3D finite difference method program.

## REFERENCES

- Dan, K., Watanabe, M., Sato, T. and Ishii, T. (2001). Short-period source spectra inferred from variable-slip rupture models and modeling of earthquake faults for strong motion prediction by semi-empirical method. *Journal of Structural and Construction Engineering. Transactions of AIJ*, **545**, 51-62 (in Japanese).
- Irikura, K. and Miyake, H. (2001). Prediction of strong ground motions for scenario earthquakes. *Journal of Geography*, **110**, 359-875 (in Japanese).
- Matsuda, T. (1975). Magnitude and recurrence interval of earthquakes from a fault. *Zisin* **2**, **28**, 269-283 (in Japanese).
- Pitarka, A. (2005). Rupture dynamics of the 1989 Loma Prieta earthquake. *Seismological Research Letters*, **76**, 252.
- Si, H. and Midorikawa, S. (1999). New attenuation relationships for peak ground acceleration and velocity considering effects of fault type and site condition. *Journal of Structural and Construction Engineering. Transactions of AIJ*, **523**, 63-70 (in Japanese).
- Somerville, P.G., Irikura, K., Graves, R., Sawada, S., Wald, D., Abrahamson, N., Iwasaki, Y., Kagawa, T., Smith, N. and Kowada, A. (1999). Characterizing crustal earthquake slip models for the prediction of strong ground motion. *Seismological Research Letters*, **70**, 59-80.
- Stirling, M., Rhoades, D. and Berryman, K. (2002). Comparison of earthquake scaling relations derived from data of the instrumental and preinstrumental era. *Bulletin of the Seismological Society of America*, **92**, 812-830.